

Intramolecular proton transfer of serine in aqueous solution. Mechanism and energetics

Francisco R. Tortonda¹, Estanislao Silla¹, Iñaki Tuñón¹, Daniel Rinaldi², Manuel F. Ruiz-López²

¹ Departamento de Química Física, Universidad de Valencia, 46100 Burjassot, Spain

² Laboratoire de Chimie Théorique, UMR CNRS-UHP 7565, Institut Nancéien de Chimie Moléculaire, Université Henri Poincaré – Nancy I, BP 239, 54506 Vandoeuvre-lès-Nancy, France

Received: 28 June 1999 / Accepted: 13 October 1999 / Published online: 14 March 2000

© Springer-Verlag 2000

Abstract. Serine amino acid in aqueous solution is theoretically studied at the B3PW91/6-31+G** level using a dielectric continuum solvent model. Neutral and zwitterionic structures in the gas phase and in solution are described and the proton-transfer mechanism is discussed. A neutral conformation in which the carboxyl hydrogen atom is already oriented toward the amino group seems to be the absolute energy minimum in the gas phase and the most stable neutral form in solution. The absolute energy minimum in solution is a zwitterionic form. The energy barrier for proton transfer is predicted to be very small, in particular when zero-point-energy contributions are added. Our calculations allow the dynamic aspects of the ionization mechanism to be discussed by incorporating nonequilibrium effects.

Key words: Proton transfer – Serine – Continuum solvent model – Nonequilibrium effects

1 Introduction

Amino acids are essential constituents of peptides and proteins. This explains the large number of studies in the literature devoted to them, in particular to investigate structural properties and tautomeric equilibria. Neutral (NE) and zwitterionic (ZW) forms may exist (and coexist) depending on the media. It is a well-known fact that some amino acids exist in NE tautomeric form in the gas phase [1–3]. This NE form can present different conformations and the assignment of the gas-phase absolute energy minimum of the simplest amino acid, glycine, was the subject of an interesting and fruitful experiment-versus-theory controversy [4–7]. In aqueous solution, hydration effects may be crucial, so conclusions reached from studies in the gas phase do not necessarily apply in that case. The solvent critically shifts the NE/

ZW tautomeric equilibrium so that the latter form becomes the absolute energy minimum in solution.

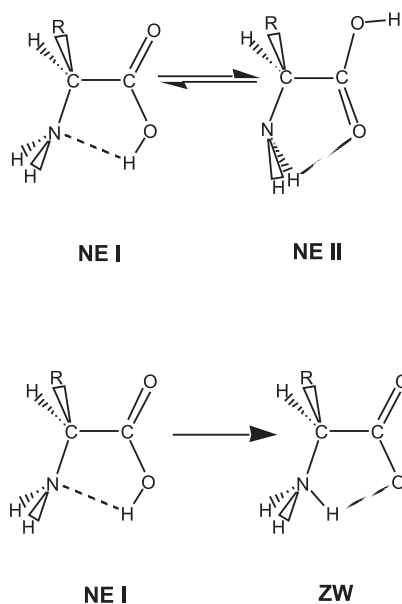
Most of the existing data on amino acid tautomeric equilibrium in solution refer to glycine. So, theoretical [8–11] and experimental [1, 2] evidence exists for the prevalence of the glycine ZW form in aqueous solution and in the solid phase. Thermodynamic and kinetic work on the tautomeric equilibrium for glycine in aqueous solution has been reported [12–15]. The free-energy difference between the ZW and the NE species has been estimated to range between 7.3 and 7.7 kcal/mol [12–14], while a measurement of the activation free energy for the ZW → NE process led to 14.6 kcal/mol [15]. Combining these values one obtains an activation free energy of roughly 7 kcal/mol for the reverse process, NE → ZW. However, comparison of kinetic and thermodynamic data is puzzling since the former suggest the activation enthalpy to be smaller than the reaction enthalpy [12–15].

Most reported computations on amino acid chemistry in solution also concern glycine [3, 8–11, 16–20]. Following these studies, a direct proton transfer from the carboxyl to the amino group seems to be the most plausible mechanism for the tautomerization process. A recent empirical valence bond (EVB) molecular dynamics simulation of the intramolecular proton transfer [21] yielded an activation free energy of 16.9 kcal/mol for the ZW → NE process and 8.4 kcal/mol for the NE → ZW one. Although the agreement with experimental data seems to be good, it appears to be fortuitous [8, 22]. Indeed, these results were obtained after parameterization of the EVB method with Hartree–Fock (HF) energies, which severely overestimate the activation barrier for this process. For instance, the computed NE → ZW activation barrier is 11.0, 2.4 and 1.9 kcal/mol at the HF, second-order Møller-Plesset (MP2) and density functional (DF) levels, respectively [8, 9] (results in aqueous solution using the 6-31+G** basis set and a solvent continuum model). Very close values have been obtained for alanine [9]. Combined DF molecular mechanics (MM) simulations have predicted a fast and very exothermic conversion of the NE to the ZW form of

Correspondence to: I. Tuñón
e-mail: ignacio.tunon@uv.es

glycine [22], in consonance with a small energy barrier for proton transfer.

More experimental and theoretical work is needed in order to clarify the apparent disagreement between experiment and theory for the activation barrier of tautomerization of glycine. A possible source of discrepancy could be found in the coupling between conformational and tautomeric equilibria in solution. The most stable NE conformation of glycine in solution differs from that in the gas phase. Let us call these conformations NE I and NE II, respectively. They have been described in previous work [8] and are represented in Scheme I. All the proton-transfer energy barrier calculations cited previously considered the NE I \rightarrow ZW process. Note that in NE I, the carboxyl and amino groups are oriented in a manner suitable for direct proton transfer; however, interpretation of experimental data of tautomeric equilibrium in solution may require both processes to be taken into account. According to our calculations [22], the conformational NE II \rightarrow NE I change in solution is expected to have a nonnegligible barrier (about 10.9 kcal/mol), whereas the proton transfer is very fast. Thus, the lifetime of NE I would be very small and, consequently, the experimentally determined activation energy of the tautomeric processes should formally be ascribed to the NE II \rightarrow ZW process and not to the proton-transfer step.



Scheme I

Here we report a study of the intramolecular proton transfer of serine in solution. The barrier and mechanism of the proton transfer depend on different factors, such as the nature of the side chain of the amino acid. In this sense, serine is a good representative of amino acids containing the complexity of a side chain capable of strong hydrogen-bonding interactions. We do not limit this study to the computation of the transition structure (TS) and the corresponding energy barrier but we also consider the dynamic aspects of the reaction by examining the role of fluctuations of the environment on the

energy profile. Consideration of these factors can be of importance to have better estimations of the proton-transfer barrier height. Previous theoretical studies on serine include protonation [23], lattice energies [24], enantiomers [25] and conformational search of the NE form in the gas phase [26–30] and of the ZW in aqueous solution [31]; however, the tautomerization process in solution has not been studied yet for this amino acid.

2 Method

Calculations were carried out using the hybrid functional B3PW91 [34] and the 6-31+G** basis set [35] (B3PW91/6-31+G**). The DF approach has previously been employed to study glycine and alanine tautomerization and results in good agreement with MP2 values were obtained [9]. It has also been successfully tested against experimental ZW vibrational spectra [9, 36]. Molecular geometries were optimized using the Bemy [37] and redundant [38] coordinate algorithms. Analytical frequency calculations were made on stationary structures in order to establish their nature (minimum or saddle point). Intrinsic reaction coordinate (IRC) calculations were carried out using the second-order Gonzalez–Schlegel integration method [39].

Solute–solvent electrostatic interactions were included into the Hamiltonian using the self-consistent reaction field (SCRf) approach of Nancy [40–42]. In the standard model, the liquid is assimilated to an isotropic polarizable medium characterized by its zero-frequency dielectric constant ($\epsilon_0 = 78.4$ for water). The quantum system (serine) is placed in a cavity whose volume is obtained from an empirical relationship [43]. The electrostatic interaction is calculated using a multipolar development of the quantum system's charge distribution. The electrostatic solvation free energy may be written as

$$\Delta G_{\text{sol}} = -\frac{1}{2} \sum_L R_L M_L,$$

where M_L are the multipole moments of the solute and R_L the reaction field components given by

$$R_L = \sum_{L'} f_{LL'}^0 M_{L'}.$$

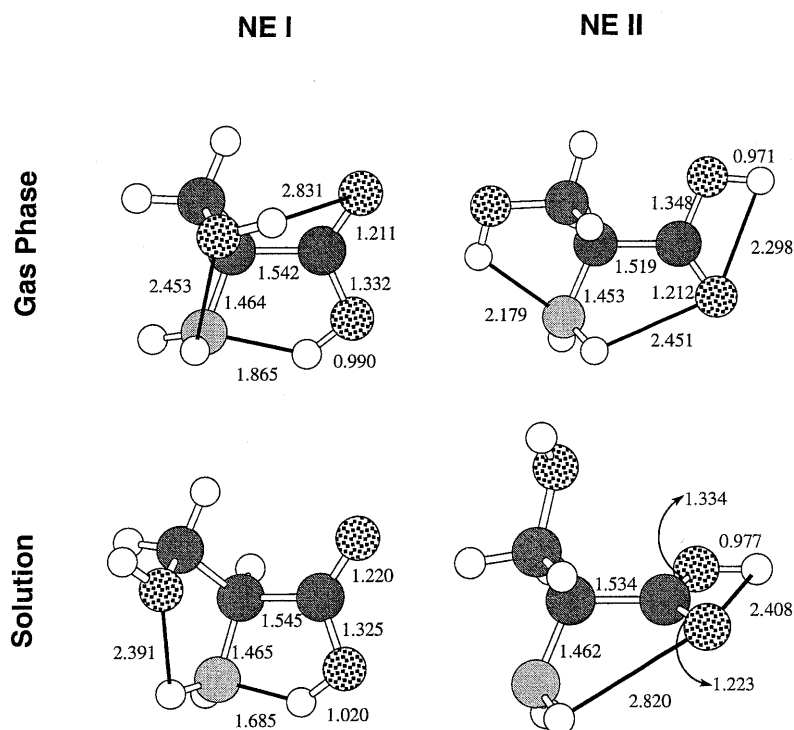
In this equation $f_{LL'}^0$ are constants that depends on ϵ_0 and the cavity definition. First and second analytical derivatives of this interaction term are easily obtained [44], allowing efficient geometry optimizations and frequency calculations.

The previous formulation is valid for evaluating static or equilibrium solvent effects. Dynamic solvent effects require the introduction of a fluctuating reaction field. For this purpose, it is useful to consider solvent polarization as having inertial and non-inertial components. The noninertial part is related to the electronic polarization of the solvent molecules and can be assumed to be always in equilibrium with the solute's charge distribution. Its value can be evaluated from the infinite-frequency relative dielectric permittivity, ϵ_∞ , (about 1.8 for water). The inertial part is related to the orientational polarization and is characterized by a large relaxation time when compared, for instance to the characteristic time for proton transfer. It is related to the difference between ϵ_0 and ϵ_∞ . If one assumes that an arbitrary inertial solvent polarization may be related to a fictitious multipole distribution, M_L^* , the solvation free energy for a system with multipoles, M_L , is [45]

$$\Delta G_{\text{sol}} = -\frac{1}{2} \sum_{LL'} f_{LL'}^0 M_{L'} M_L + \frac{1}{2} \sum_{LL'} (f_{LL'}^0 - f_{LL'}^\infty) \Delta M_{L'} \Delta M_L,$$

where $\Delta M_L = M_L - M_L^*$. Note the presence of f factors for both dielectric constants. The first term in the expression is the equilibrium free energy, whereas the second is a positive destabilizing term representing the non-equilibrium contribution. In principle, M_L^* may take any value, but only some particular cases have physical interest (see later).

Fig. 1. Optimized structures of the neutral (*NE*) conformers NE I and NE II of serine in the gas phase and in solution. *Bond lengths* are given in angstroms



For simpleness, we assume that the cavity shape is constant along the proton-transfer reaction coordinate, which seems to be a reasonable approximation (the estimated cavity volume change is only about 1%). This assumption justifies the use of a simple ellipsoidal cavity shape. The multipole development is made up to the sixth order, ensuring a good convergence of the solvation energy.

All calculations were carried out using the Gaussian94 program [46] interfaced with software developed at Nancy [47] for solvent effects.¹ It should be finally mentioned that our calculations do not include two important factors that could partially change the present results: the quantum nature of the proton motion and specific solute-solvent interactions. About this last point, a recent investigation on glycine tautomerization [8] has shown that water molecules probably do not actively participate in the proton transfer.

3 Results

We first summarize the results for the structure of serine in solution. We describe the stationary points predicted for NE and ZW forms as well as for the TS leading to proton transfer. The corresponding IRC is described. The role of fluctuations of the system on the energy profile is incorporated afterwards.

3.1 NE amino acid conformations

We start the present study with the analysis of the NE form of serine. From previous studies on other amino acids [8, 9] and considering the results obtained for serine in the gas phase [30], we selected the two conformers NE I and NE II as candidates to be the

absolute energy minimum for the NE form. The B3PW91/6-31+G** optimized structures of both conformers in the gas phase and in solution are shown in Fig. 1.

Let us first consider the gas-phase structures. NE I displays a cycliclike conformation where the carboxyl and amino groups form an intramolecular hydrogen bond. In NE II, the carboxyl group has rotated 180° around the C—C bond. This conformation has been reported to be the absolute gas-phase energy minimum for glycine, alanine and serine [8, 9, 17, 30]. In the latter case, the energy difference with respect to NE I was predicted to be only 0.1 kcal/mol through MP2/6-31+G* energy computations using RHF geometries and 0.3 kcal/mol at the MP4SDQ/6-31+G**/MP2 level [30]. At the present computational level, we also predict a small energy difference, but the NE I structure is found to be more stable than NE II by 0.42 kcal/mol in the gas phase (0.21 kcal/mol if we include zero-point energies). Though the relative order seems to be quite sensitive to the computational level, the absolute energy difference is always small, as illustrated by the following values: ΔE (NE II – NE I) = 0.16, 0.44 and –0.02 kcal/mol at MP2/6-31+G**, B3PW91/6-311++G** and MP2/6-311++G** levels, respectively. The smaller energy difference in serine with respect to that in glycine and alanine can be attributed to a cooperativity effect between intramolecular hydrogen bonds in which the hydroxyl group participates. In NE I, the hydroxyl group forms two hydrogen bonds, one acting as a proton donor with the carbonyl oxygen and the other one as a proton acceptor with the amino group, while in NE II, the hydroxyl group only forms one hydrogen bond with the amino group. Thus, the cooperativity effect is expected to favor NE I with respect to NE II.

¹ The software developed at Nancy was modified by D. Rinaldi

In solution, we find the same picture as in previously studied amino acids. Because of the larger dipole moment of NE I (8.82 D versus 0.83 D for NE II), the energy gap (now including the electrostatic and polarization free energy of solvation, ΔG_{sol}) between both NE structures is considerably increased and now NE I is 4.02 kcal/mol more stable than NE II (3.73 kcal/mol taking into account zero-point energies). It is worthwhile to make a few remarks concerning the geometrical changes induced by solvent effects on the NE structures. First, one notes that, in contrast to the gas phase, the hydroxyl hydrogen atom does not form an intramolecular hydrogen bond. The hydrogen atom is now oriented toward the solvent, favoring the solute interaction with its solvent environment. The energy cost of keeping the intramolecular hydrogen bond can be estimated to amount to about 1.0 kcal/mol. Besides, it may be noted that in structure NE II the carboxyl group lies on a plane perpendicular to the NCC one (while in the gas phase both groups were found to lie on the same plane). It has already been discussed [9] that solvent effects diminish the force constant associated with this movement and thus the carboxyl group would be able to rotate in order to optimize its interactions with the solvent. One should also note that the breaking of the cyclic intramolecular hydrogen-bond network by solvent effects is compensated by the cooperativity between intramolecular hydrogen bonds and electrostatic solute-solvent interactions [43]. Finally, it must be noted that in NE I, the hydrogen bond between the hydrogen atom in the carboxyl group and the amino group is favored by the solvent. The OH and NH distances in the gas phase are 0.990 and 1.865 Å, respectively, while in solution they are 1.020 and 1.685 Å. This effect leads, in turn, to a reinforcement of the hydrogen bond of the amino group with the hydroxyl oxygen. These geometric changes, together with the polarization of the electronic cloud, contribute to a large increase in the dipole moment when passing from the gas phase (4.34 D) to solution (8.82 D). The introduction of specific solute-solvent interactions could slightly change the current description of solvent effects on the intramolecular hydrogen bonds; however, the more important trends are usually well given by the continuum model.

3.2 Zwitterion

Attempts to locate a ZW minimum-energy structure in the gas phase at the current computational level always failed. The ZW structure in solution is displayed in Fig. 2. As shown by comparing this structure to those in Fig. 1, proton transfer from the carboxyl to the amino group does not produce very important geometrical changes. The intramolecular hydrogen bond between the amino group and the hydroxyl oxygen atom is reinforced as a consequence of the positive charge developed on the amino group. In the carboxyl group, the carbonyl double bond is now delocalized between the two oxygen atoms and the two CO distances become quite similar. The calculated bond lengths agree quite well with the experimental neutron diffraction values determined from serine monohydrate crystals [48]. Typical deviations are

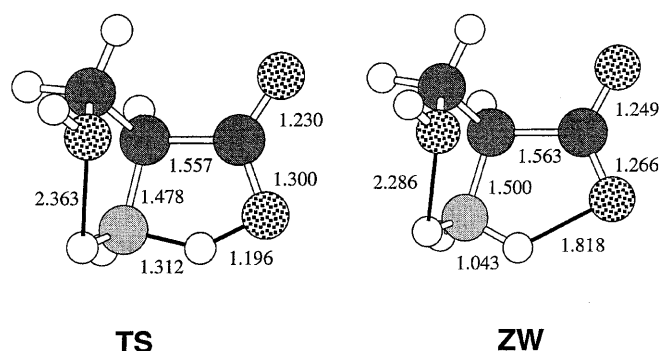


Fig. 2. Optimized structures of the zwitterionic (ZW) form of serine and the transition structure (TS) connecting with the NE form in solution. Bond lengths are given in angstroms

about ± 0.01 Å, except for the CC_α distance which is 0.03 Å shorter in the crystal.

3.3 Energetics and reaction path

The TS for proton transfer from NE I to ZW in solution (assuming solute-solvent equilibrium) was directly located on the potential-energy surface (which includes the electrostatic and polarization free energy) starting from an initial guess structure derived from our previous work on glycine and alanine and using an analytical Hessian matrix. The computed geometry is given in Fig. 2. After optimization, we carried out an analytical frequency calculation and verified that the proposed structure had one imaginary value ($999.7i \text{ cm}^{-1}$). In the TS the OH distance is still shorter than the NH one. The OH bond has been lengthened by about 0.18 Å while the NH bond has been shortened by 0.37 Å, which is mainly due to the reduction of the NO distance.

Relative energies of the structures studied, with and without consideration of the zero-point-energy contributions, are given in Table 1. The ZW form is more stable than the NE one in solution by about 3 kcal/mol (2 kcal/mol if we take into account zero-point energies). It has been previously discussed [9] that this energy difference could be underestimated and that the model should be refined to get more reliable relative energies between the two tautomeric forms in solution.

The calculated energy barrier for proton transfer is 1.40 kcal/mol (0.44 kcal/mol after zero-point-energy correction) which is not far from the barrier found for

Table 1. Relative energies (kcal/mol), with and without inclusion of zero-point energy (ZPE) contributions, of the neutral (NE) structures, the transition structure (TS) and the zwitterionic (ZW) structure studied at the B3PW91/6-31+G** level assuming equilibrium solvation. Values in parentheses are gas-phase energies

	ΔE	$\Delta(E + \text{ZPE})$
NE II	4.02 (0.42)	3.73 (0.21)
NE I	0.00	0.00
TS	1.40	0.44
ZW	-2.95	-2.00

glycine at the same level. This energy barrier can be easily overpassed at room temperature and thus one could consider proton transfer in serine as a nearly barrierless process (if solute–solvent equilibrium conditions are assumed, see later for nonequilibrium effects).

The IRC pathways, from the TS down to the reactant (NE I) and product (ZW) valleys have been traced. From the last point of the IRC calculation toward the products we started a geometry optimization that led to the ZW form. The reaction profile in solution is shown in Fig. 3. For comparison, Fig. 3 also shows the energies obtained for the isolated reaction system using the structures along the solution reaction path. The solute reaction coordinate, r_s , ranges from -1.4 au (NE I) to 2.0 au (ZW). As usual, the TS is defined as the structure having $r_s = 0$. The whole proton-transfer process can be decomposed in three schematic phases. First, the proton donor–proton acceptor (NO) distance is reduced from 2.494 Å to a value close to that found in the TS (2.374 Å). Then, proton transfer from oxygen to nitrogen occurs with a nearly constant NO distance. Finally, the NO distance lengthens to its final value in the ZW 2.558 Å.

3.4 Dynamic effects

The previous reaction path assumes the equilibrium hypothesis, i.e., all the solute and solvent degrees of freedom are fully relaxed for a given value of the reaction coordinate, the latter being defined by a combination of solute coordinates. Actually, proton transfer is a very fast process which takes only a few tens of femtoseconds (see, for example, the DF/MM molecular dynamics simulation in Ref. [22]) and the equilibrium hypothesis does not hold in practice. For instance, solvent orientational relaxation lies on the picosecond scale and is much slower than the reaction event. In this part, we discuss how nonequilibrium situations may affect the proton transfer mechanism. The general idea is to assume that the reaction can

proceed for suitable configurations of the solute–solvent system that remain essentially frozen during the transfer of the proton. Obviously, only some cases present physical interest, namely those configurations accessible by thermal fluctuations. The importance of environment fluctuations has been demonstrated for proton transfer in solution and also for enzymatic reactions [49–51]. A full dynamic treatment would be necessary in order to investigate formally these fluctuations and a few recent works have addressed this specific point [21, 22]. In the SCRf model, one can simply draw a schematic picture by including nonequilibrium energy corrections in the static treatment [45], following original ideas by Marcus [52] and Kurz and Kurz [53] and developed by other authors [50, 54].

Let us first consider the solvent degrees of freedom. To a first approximation, one may consider that the inertial solvent polarization, P^i , is frozen during the reaction whereas the noninertial component P^{ni} , relaxes instantaneously and is in equilibrium with the chemical system [33]. At the reactants, P^i fluctuates around a mean value with probabilities given by the corresponding Boltzmann factor. Among all possible fluctuations, those that favor the solvation of the ZW form are expected to assist proton transfer. This is shown in Fig. 4, where we have plotted the energy profile for the reaction path by assuming different values of a global solvent coordinate, s , that corresponds to the inertial polarization of equilibrated configurations of the system at particular locations along the reaction coordinate: the NE form ($s = -1.4$ au), the TS ($s = 0.0$ au), the final ZW ($s = 2.0$ au) and an intermediate structure ($s = -0.7$ au). The equilibrium curve is also plotted for comparison. For the “reactant-like” profile ($s = -1.4$ au) the energy maximum is shifted toward the product side and the effective energy barrier is higher than in the equilibrium case, namely 2.8 kcal/mol. There is still a ZW energy minimum on the profile but it is shifted toward smaller values of the reaction coordinate. Besides, the NE form is now 1.98 kcal/mol more stable than the ZW and the barrier for the reverse process is small (0.8 kcal/mol). Obviously, this case does not favor charge

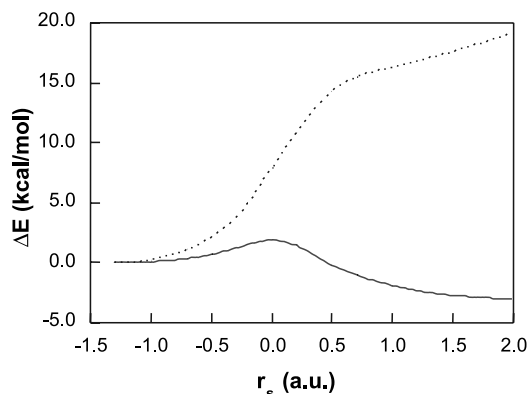


Fig. 3. Energy profile of the intramolecular proton transfer process of serine (NE → ZW) in solution. The *continuous line* corresponds to the total energy in solution and the *dashed line* to the gas-phase energy of the structures appearing along the intrinsic reaction coordinate obtained in solution

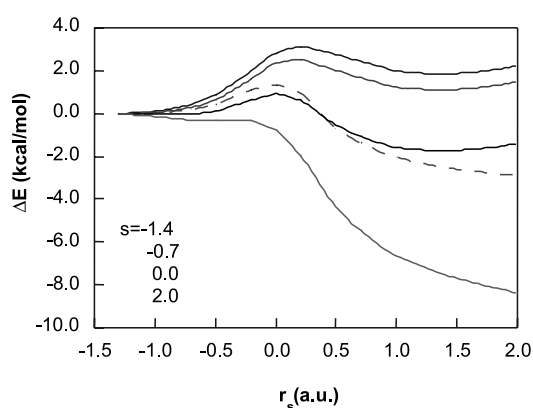


Fig. 4. Energy profiles of the intramolecular proton transfer process of serine (NE → ZW) in solution at different nonequilibrium conditions ($s = -1.4, -0.7, 0.0, 2.0$ au). The equilibrium curve (*dashed line*) is also included for comparison

separation. By increasing s , the ZW form is progressively stabilized with respect to the NE form and the energy barrier decreases. It vanishes for the “product-like” profile ($s = 2.0$ au).

We now consider the solute degrees of freedom. For simplicity, we only select an internal coordinate which is closely related to the barrier height: the NO distance, d_{NO} . Previous DF/MM molecular dynamics simulations for glycine in water at 25 °C showed the NO distance in the NE conformer to oscillate by more than 0.3 Å [22]. On the other hand, in serine, the potential energy of NE I displays only modest energy changes with respect to d_{NO} . For instance, shortening d_{NO} from 2.494 Å (i.e., the value for the minimum-energy structure) to 2.380 Å (which is close to the value for the TS in Fig. 2) requires only 0.72 kcal/mol. This is a striking result as far as diminishing the NO distance renders easier proton transfer, so for $d_{\text{NO}} = 2.33$ Å a barrierless transfer is predicted.

Let us now discuss the energetics of proton transfer in a few relevant solute–solvent nonequilibrium configurations. We computed the energy profiles in the following way. First we selected three values of the NO distance $d_{\text{NO}} = 2.38, 2.45$ and 2.50 Å, the first and the last values being close to those found, respectively, in the TS and the NE conformer of the equilibrium scenario. The geometry of NE I is relaxed in solution as usual but the NO constraint is kept. From the resulting geometry, we performed a scan of the proton position maintaining the NO distance constant. The reaction coordinate is simply the difference $d_{\text{OH}} - d_{\text{NH}}$. For each NO value, we computed the energy profile using a frozen inertial solvent polarization which is either “reactant-like” or “TS-like”. Relative energy profiles are plotted in Fig. 5 (note that the energy reference is the NE structure NE I in equilibrium solvation). As a function of the fluctuating quantities considered, the upper point of the energy profiles changes substantially. It varies between 1.5 and 5.5 kcal/mol. The highest value corresponds to $d_{\text{NO}} = 2.50$ Å and “reactant-like” solvent polarization. The lowest value holds for $d_{\text{NO}} = 2.38$ and “TS-like” solvent polarization. The fact that proton transfer is favored by a NO length decrease and forward solvent fluctuations was expected on the basis of the comments made previously. The most striking information contained in Fig. 5 is that the energy cost to get a suitable non-equilibrium solute–solvent configuration assisting proton transfer is small (around 1 kcal/mol). Such a fluctuation is of the order of kT and is accessible at usual temperatures. Therefore, the proton transfer in serine can take place through this frozen-environment mechanism that requires an energy cost comparable to that found for the ideal fully relaxed environment one.

4 Conclusions

In contrast to glycine and alanine amino acids, the gas-phase serine NE structures NE I and NE II are very close in energy, but further theoretical calculations and experimental work are necessary in order to determine unambiguously their relative energy. In aqueous solution, NE I is found to be the absolute energy

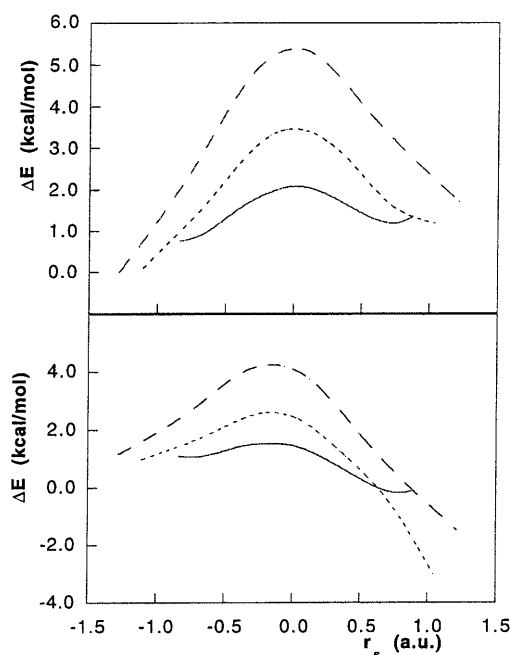


Fig. 5. Energy profiles of the intramolecular proton transfer process of serine (NE → ZW) in solution at different nonequilibrium conditions for both the solvent and the solute coordinates. The upper figure corresponds to a frozen solvent at the reactants and the bottom figure to frozen solvent at the TS. The different lines represent different fixed N–O distances. Continuous line: 2.38 Å, short dashed line: 2.45 Å, long dashed line: 2.50 Å

minimum for the NE form, in accordance with the results found for glycine and alanine. The reason is basically the much larger dipole moment of NE I compared to that of NE II. The NE/ZW tautomeric conversion has also been studied. There is not a stable ZW in the gas phase. In solution, the ZW form is about 2–3 kcal/mol more stable than the NE form but, as discussed previously [9], this energy difference could be somewhat underestimated. The equilibrium proton-transfer path leading from NE serine to its ZW shows a small energy barrier (1.4 kcal/mol) which nearly disappears when considering zero-point energies. Thus, under equilibrium conditions, NE I will quickly undergo proton transfer to give the corresponding serine ZW.

According to the conclusions of previous investigations on proton transfer in solvated systems, dynamical or nonequilibrium effects can be important. The energy shift of the energy barrier due to the lack of solvent relaxation reaches 3 kcal/mol, but this value can change and may even become negative when appropriate solvent fluctuations are taken into consideration. The study of dynamical effects has been extended here to the solute’s degrees of freedom, in particular, to the proton donor–proton acceptor distance d_{NO} , which can largely determine the magnitude of the energy barrier. We have compared proton-transfer energy profiles for different values of d_{NO} and solvent inertial polarization (both kept frozen along the reaction path). We found that for $d_{\text{NO}} = 2.38$ and “TS-like” solvent polarization, the proton transfer is extremely favorable with a negligible activation barrier. The energy cost for reaching such a

solute–solvent configuration is of the order of kT at room temperature and is therefore accessible to the hydrated serine system.

Acknowledgements. This work was started during a short visit of I. T. to the Laboratoire de Chimie Theorique (Nancy) supported by the Generalitat Valenciana Project GVDOC98-CB-11-8. It has been partly supported by DGICYT Project PB96-0792. I. T. acknowledges a postdoctoral contract of the Ministerio de Educación y Ciencia (Spain) and the Universitat de Valencia. The authors acknowledge A. G. Császár for providing them with a copy of his paper to appear in *Progress in Biophysics and Molecular Biology*.

References

- Albrecht G, Corey RB (1939) *J Am Chem Soc* 61: 1087
- Jonsson PG, Kvik A (1972) *Acta Crystallogr Sect B* 28: 1827
- Ding Y, Krogh-Jespersen K (1992) *Chem Phys Lett* 199: 261
- Vishveshwara S, Pople JA (1977) *J Am Chem Soc* 99: 2422
- Brown RD, Geoffrey PD, Storey JWV, Bassez MP (1978) *J Chem Soc Chem Commun* 547
- Sellers HL, Schäfer L (1978) *J Am Chem Soc* 100: 7728
- Schäfer L, Sellers HL, Lovas FJ, Suenram RD (1980) *J Am Chem Soc* 102: 6568
- Tortonda FR, Pascual-Ahuir JL, Silla E, Tuñón I (1996) *Chem Phys Lett* 260: 21
- Tortonda FR, Pascual-Ahuir JL, Silla E, Tuñón I, Ramírez FJ (1998) *J Chem Phys* 109: 592
- Bonaccorsi R, Palla P, Tomasi J (1984) *J Am Chem Soc* 106: 1945
- Andzelm J, Kölmeland C, Klamt A (1995) *J Chem Phys* 21: 9312
- Wada G, Tamura E, Okina M, Nakamura M (1982) *Bull Chem Soc Jpn* 55: 3064
- Haberfield PJ (1980) *J Chem Educ* 57: 346
- Edsall JT, Blanchard MH (1933) *J Am Chem Soc* 55: 2337
- Slifkin MA, Ali SM (1984) *J Mol Liq* 28: 215
- Hu CH, Shen M, Schaefer HF III (1993) *J Am Chem Soc* 115: 2923
- Császár AG (1995) *THEOCHEM* 346: 141
- Romano S, Clementi E (1978) *Int J Quantum Chem* 14: 839
- Alagona G, Ghio C, Kollman PA (1988) *THEOCHEM* 166: 385
- Jensen JH, Gordon MS (1995) *J Am Chem Soc* 117: 8159
- Okuyama-Yoshida N, Nagaoka M, Yamabe T (1998) *J Phys Chem* 102: 285
- Tuñón I, Silla E, Millot C, Martins-Costa MTC, Ruiz-López MF (1998) *J Phys Chem A* 102: 8673
- Mezey PG, Ladik JJ, Suhai S (1979) *Theor Chim Acta* 51: 323
- Voogd J, Derissen JL, van Duijneveldt FB (1981) *J Am Chem Soc* 115: 8321
- Tranter GE (1985) *Mol Phys* 4: 825
- Van Alsenoy C, Scarsdale JN, Sellers HL, Schäfer L (1981) *Chem Phys Lett* 80: 124
- Masamura M (1988) *THEOCHEM* 164: 299
- Van Alsenoy C, Kulp S, Siam K, Klimkowski J, Ewbank JD, Schäfer L (1988) *THEOCHEM* 181: 169
- Tarakeshwar P, Manogaran S (1994) *THEOCHEM* 305: 205
- Gronert S, O'Hair RA (1995) *J Am Chem Soc* 117: 2071
- Kikuchi O, Takayuki M, Sawahata H, Takahashi O (1994) *THEOCHEM* 305: 79
- Tuñón I, Martins-Costa MTC, Millot C, Ruiz-López MF (1997) *J Chem Phys* 106: 3633
- Ruiz-López MF, Oliva A, Tuñón I, Bertrán J (1998) *J Phys Chem A* 102: 10728
- (a) Becke AD (1988) *Phys Rev A* 38: 3098; (b) Perdew JP, Wang Y (1992) *Phys Rev B* 45: 13244
- (a) Hariharan PC, Pople JA (1973) *Theor Chim Acta* 28: 213; (b) Clark T, Chandrasekhar J, Spitznagel GW, Schleyer PvR (1983) *J Comput Chem* 4: 294
- Ramírez FJ, Tuñón I, Silla E (1998) *J Phys Chem B* 102: 6290
- Schlegel HB (1982) *J Comput Chem* 3: 214
- Peng C, Ayala PY, Schlegel HB, Frisch MJ (1996) *J Comput Chem* 17: 49
- (a) Fukui K (1970) *J Phys Chem* 74: 4161; (b) Gonzalez C, Schelegel HB (1990) *J Phys Chem* 94: 5523; (c) Gonzalez C, Schelegel HB (1991) *J Chem Phys* 95: 5853
- Rinaldi D, Rivail JL (1973) *Theor Chim Acta* 32: 57
- Rivail JL, Rinaldi D (1976) *Chem Phys* 18: 233
- Rivail JL, Rinaldi D, Ruiz-López MF (1991) In: Formosinho SJ, Arnaut L, Csizmadia I (ed) *Theoretical and computational models for organic chemistry*. Kluwer, Dordrecht, pp 79–92
- Bertrán J, Ruiz-López MF, Rinaldi D, Rivail JL (1992) *Theor Chim Acta* 84: 181
- Rinaldi D, Rivail JL, Rguini N (1992) *J Comput Chem* 13: 675
- Ruiz-López MF, Rinaldi D, Bertrán J (1995) *J Chem Phys* 103: 9249
- Frisch MJ, Trucks GW, Schlegel HB, Gill PMW, Johnson BG, Robb MA, Cheeseman JR, Keith T, Petersson GA, Montgomery JA, Raghavachari K, Al-laham MA, Zakrzewski VG, Ortiz JV, Foresman JB, Cioslowski J, Stefanov BB, Nanayakkara A, Challacombe M, Peng CY, Ayala PY, Chen W, Wong MW, Andres JL, Replogle ES, Gomperts R, Martin RL, Fox DJ, Binkley JS, Defrees DJ, Baker J, Stewart JP, Head-Gordon M, Gonzalez C, Pople JA (1995) *Gaussian* 94, revision D3. Gaussian, Pittsburgh, Pa
- Rinaldi D, Pappalardo PP (1992) QCPE program no 622
- Frey MN, Lehmann MS, Koetzle TF, Hamilton WC (1973) *Acta Cryst B* 29: 876
- (a) Warshel A (1984) *Proc Natl Acad Sci USA* 81: 444; (b) Warshel A, Sussman F, Hwang JK (1988) *J Mol Biol* 201: 139; (c) Warshel A (1991) *Computer modeling of chemical reactions in enzymes and solutions*. John Wiley & Sons, New York
- Timoneda JJ, Hynes JT (1991) *J Phys Chem* 95: 10431
- (a) Kramers HA (1940) *Physica* 7: 284; (b) Marcus RA (1956) *J Chem Phys* 24: 966
- Marcus RA (1956) *J Chem Phys* 24: 979
- Kurz JL, Kurz LC (1972) *J Am Chem Soc* 94: 4451
- (a) Kim HJ, Hynes JT (1992) *J Am Chem Soc* 114: 10508; (b) Kim HJ, Hynes JT (1992) *J Am Chem Soc* 114: 10528; (c) Bianco R, Miertus S, Persico M, Tomasi J (1992) *Chem Phys* 168: 281; (d) Aguilar M, Bianco R, Miertus S, Persico M, Tomasi J (1993) *Chem Phys* 174: 397; (e) Aguilar MA, Olivares del Valle FJ, Tomasi J (1993) *J Chem Phys* 98: 7375; (f) Basilevsky MV, Chudinov GE, Napolov DV (1993) *J Phys Chem* 97: 3270; (g) Aguilar MA, Hidalgo A (1995) *J Phys Chem* 99: 4293